View metadata, citation and similar papers at core.ac.uk

brought to you by CORE

provided by Tamkang University Institutional Repository

Fast growth of ultrananocrystalline diamond films by bias-enhanced nucleation and growth process in CH4/Ar plasma

A. Saravanan, B. R. Huang, K. J. Sankaran, C. L. Dong, N. H. Tai, and I. N. Lin

Citation: Applied Physics Letters **104**, 181603 (2014); doi: 10.1063/1.4875808

View online: http://dx.doi.org/10.1063/1.4875808

View Table of Contents: http://scitation.aip.org/content/aip/journal/apl/104/18?ver=pdfcov

Published by the AIP Publishing

Articles you may be interested in

Origin of graphitic filaments on improving the electron field emission properties of negative bias-enhanced grown ultrananocrystalline diamond films in CH4/Ar plasma
J. Appl. Phys. **116**, 163102 (2014); 10.1063/1.4899245

Microwave plasma enhanced chemical vapor deposition of nanocrystalline diamond films by bias-enhanced nucleation and bias-enhanced growth
J. Appl. Phys. **115**, 024308 (2014); 10.1063/1.4861417

Ultrananocrystalline diamond nano-pillars synthesized by microwave plasma bias-enhanced nucleation and bias-enhanced growth in hydrogen-diluted methane
J. Appl. Phys. **112**, 124307 (2012); 10.1063/1.4769861

Bias-enhanced nucleation and growth processes for improving the electron field emission properties of diamond films
J. Appl. Phys. **111**, 053701 (2012); 10.1063/1.3687918

Effect of pretreatment bias on the nucleation and growth mechanisms of ultrananocrystalline diamond films via bias-enhanced nucleation and growth: An approach to interfacial chemistry analysis via chemical bonding mapping
J. Appl. Phys. **105**, 034311 (2009); 10.1063/1.3068366

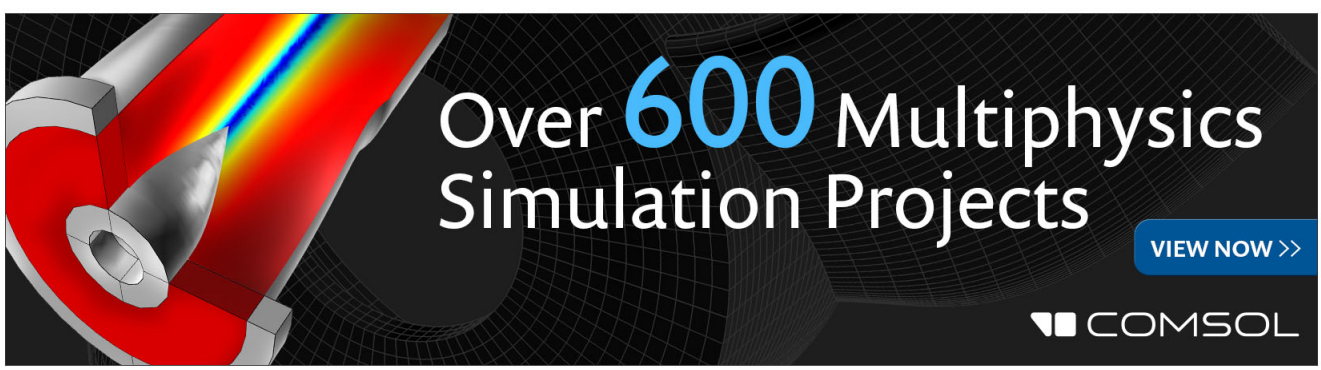

This article is copyrighted as indicated in the article. Reuse of AIP content is subject to the terms at: http://scitation.aip.org/termsconditions. Downloaded to IP: 163.13.36.166 On: Fri, 12 Dec 2014 02:24:24

Fast growth of ultrananocrystalline diamond films by bias-enhanced nucleation and growth process in CH_4/Ar plasma

A. Saravanan,[1] B. R. Huang,[1] K. J. Sankaran,[2] C. L. Dong,[3] N. H. Tai,[2] and I. N. Lin[4,a)]
[1]*Graduate Institute of Electro-Optical Engineering and Department of Electronic Engineering, National Taiwan University of Science and Technology, Taipei 106, Taiwan*
[2]*Department of Materials Science and Engineering, National TsingHua University, Hsinchu 300, Taiwan*
[3]*Scientific Research Division, National Synchrotron Radiation Research Center, Hsinchu 300, Taiwan*
[4]*Department of Physics, Tamkang University, Tamsui 251, Taiwan*

(Received 21 March 2014; accepted 28 April 2014; published online 7 May 2014)

This letter describes the fast growth of ultrananocrystalline diamond (UNCD) films by bias-enhanced nucleation and growth process in CH_4/Ar plasma. The UNCD grains were formed at the beginning of the film's growth without the necessity of forming the amorphous carbon interlayer, reaching a thickness of ~380 nm in 10 min. Transmission electron microscopic investigations revealed that the application of bias voltage induced the formation of graphitic phase both in the interior and at the interface regions of UNCD films that formed interconnected paths, facilitating the transport of electrons and resulting in enhanced electron field emission properties. © *2014 AIP Publishing LLC*. [http://dx.doi.org/10.1063/1.4875808]

The admirable properties of diamond, namely, high hardness, low friction coefficient, chemical inertness, high electrical resistivity, and semiconducting properties makes it a promising material for numerous applications.[1–3] Ultrananocrystalline diamond (UNCD) films grown in CH_4/Ar plasma possess nano-sized grains with grain boundaries of considerable thickness, which contain sp^2-bonds and hence acquire excellent conductivity.[4] The transport of electrons through the UNCD films is noticeably better than the conventional microcrystalline diamond (MCD) films and therefore the UNCD films possess superior electron field emission (EFE) properties than the MCD films.[5,6] However, the conductivity of grain boundary phase in UNCD films is still poor which hinders the performance of the EFE emitters made from UNCD films. Moreover, nucleation of diamond grains on Si substrates is difficult. The formation of an amorphous carbon (*a-C*) phase as transition layer between the dissimilar materials is usually required.[7] Such an *a-C* layer is rather resistive and hinders the transport of electrons from Si to UNCD films thereby limiting the EFE properties attainable in UNCD films.

The bias-enhanced nucleation and growth (BEN-BEG) process is found to be an effective diamond nucleation technique, which can circumvent the formation of *a-C* films for MCD films grown in CH_4/H_2 plasma.[8] The application of bias voltage in the CH_4/H_2 plasma using microwave plasma enhanced chemical vapor deposition (MPECVD) system not only facilitated the growth of diamond but also efficiently reduced the size of the grains.[9,10] Moreover, Teng *et al.* reported the enhanced EFE behavior for the BEG grown diamond films in CH_4/H_2 plasma and proposed that BEG process can convert the *a-C* into nanographite phases.[11] Nevertheless, whether the same BEN-BEG process can be applied in CH_4/Ar plasma for growing the UNCD films has not been reported yet.

In this paper, we report on the high growth rate of UNCD films achieved by applying negative bias voltage in CH_4/Ar plasma. The application of negative bias initiated the formation of UNCD grains even in the minimum growth time of 10 min. In addition, the bias voltage induced the formation of graphitic phases in the interior and the interface of UNCD films that enhanced the electron conduction, resulting in the improved EFE properties.

The UNCD films were grown on *n*-type silicon substrates by MPECVD system. Prior to the deposition of UNCD films, the silicon substrates were preseeded by ultrasonication in methanol solution, containing nano-sized diamond powders (~5 nm) and Ti powders (~32.5 nm) for 45 min. The substrates were ultrasonicated again in methanol for 1 min to eradicate the possibly adhered nanoparticles. The UNCD films were grown in Ar (98%)/CH_4 (2%) plasma (100 sccm) and excited by a 1200 W microwave power with a 150 Torr total pressure. A negative bias voltage (−200 V) was applied to the Si substrate when the pressure reached 150 Torr. It should be noted that unlike the case in the CH_4/H_2 plasma, in which applying a negative voltage is straightforward and very effective in modifying the granular structure of the MCD films, the application of bias voltage in CH_4/Ar plasma is rather difficult, as the arcing is easily induced in the Ar plasma. We re-designed the stainless steel substrate holder to a square shaped holder with roundish in edges, in which the Si-substrate is accommodated almost in plane with the surface of the substrate holder. The films were grown for 10 min and the corresponding films were designated as $UNCD_{10B}$. In addition, the UNCD films without bias of different growth periods (10 and 30 min) were grown to facilitate the comparison and the corresponding films were designated as $UNCD_{10N}$ and $UNCD_{30N}$, respectively.

The bias current is an effective parameter that can monitor the progress of the nucleation of diamond in the BEN-BEG process. The top right inset of Fig. 1(a) shows the evolution of bias current against the time after the onset of the application of the negative bias voltage. The bias current

a)Electronic mail: inanlin@mail.tku.edu.tw

 © 2014 AIP Publishing LLC

This article is copyrighted as indicated in the article. Reuse of AIP content is subject to the terms at: http://scitation.aip.org/termsconditions. Downloaded to IP: 163.13.36.166 On: Fri, 12 Dec 2014 02:24:24

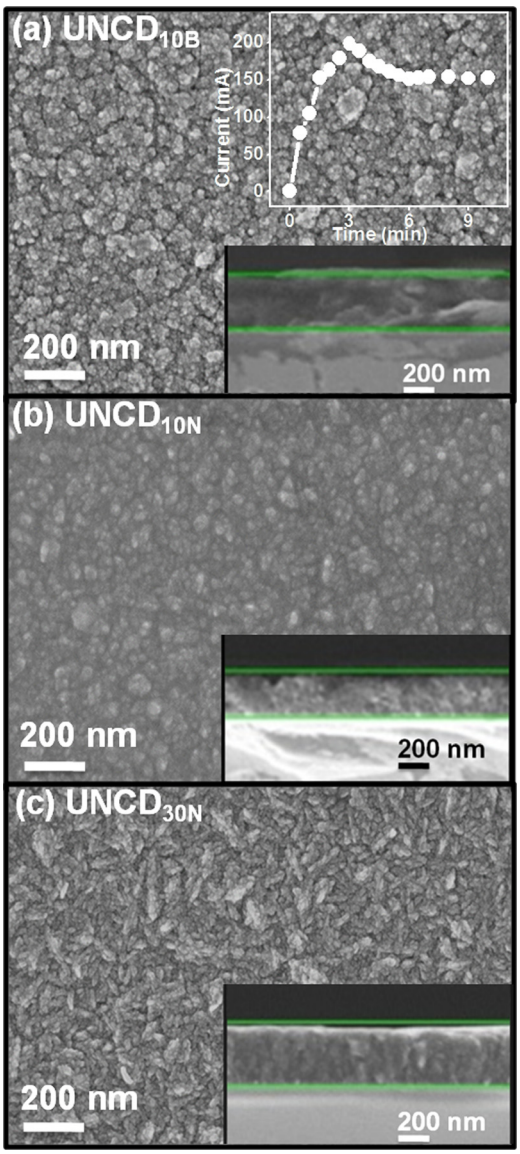

FIG. 1. SEM micrographs with the insets showing the cross-sectional SEM image of (a) $UNCD_{10B}$, (b) $UNCD_{10N}$, and (c) $UNCD_{30N}$ films. The evolution of bias current in negative bias of −200 V is shown in the top right inset of Fig. 1(a).

increased rapidly and reached a saturated value of 200 mA/cm^2 in 3 min after the application of bias voltage, indicating that the diamond nuclei have already fully covered the Si substrates in such a short interval. It is to be mentioned that in CH_4/H_2 plasma, the bias current required at least 7.5 min to reach a saturated value.[11] Fig. 1(a) shows scanning electron microscopy (SEM; Jeol JSM-6500F) image of the $UNCD_{10B}$ films. The morphology of the $UNCD_{10B}$ shows random and spherically structured grains in the films (Fig. 1(a)), with the thickness of ∼380 nm, which was estimated from the cross-sectional SEM micrographs of the films (bottom right inset of Fig. 1(a)). The growth rate was around ∼38 nm/min. In contrast, when the films were grown without the negative bias voltage, the growth rate of $UNCD_{10N}$ films decreased markedly to around 22 nm/min., i.e., with thickness of ∼220 nm when grown without bias in CH_4/Ar plasma for 10 min (inset of Fig. 1(b)). The granular structure has not yet completely developed and the films contain large proportion of *a-C* phase (Fig. 1(b)). The detailed microstructural investigation on these UNCD films will be further illustrated using transmission electron microscopy (TEM) shortly. It requires at least 30 min in MPECVD process without bias to develop a spherically granular structured as similar to that of the morphology of $UNCD_{10B}$ films ($UNCD_{30N}$, Fig. 1(c)). Moreover, the $UNCD_{30N}$ films show the thickness of ∼330 nm with average growth rate of ∼11 nm/min (inset of Fig. 1(c)). From these observations, we can conclude that by applying −200 V bias, we obtained several fold of magnitude higher growth rate for UNCD films grown in CH_4/Ar plasma, as compared to the films grown without bias.

For the purpose of explicitly differentiating the various types of carbon bonding configuration in the films, near edge X-ray absorption spectroscopy (NEXAFS) for these UNCD films were examined. Fig. 2 shows the NEXAFS spectra of the UNCD films deposited in CH_4/Ar plasma with and without bias. Curve I in Fig. 2 clearly ascertains that the major configuration of carbon in $UNCD_{10B}$ films is the sp^3-bonded carbon of the diamond phase, with a smaller amount of sp^2-bonded carbons distributed in the films.[12,13] A sharp peak at ∼289.5 eV corresponds to the electron core excitation of C-C (1s)-σ^* of the sp^3-bonded carbon in diamond, whereas a dip valley observed at 302.0 eV is assigned to the second absorption band gap of diamond.[14,15] The small peak at ∼284.5 eV is assigned to the C1s-π^* transition corresponding to the sp^2 phase.[16,17] Moreover, a weak bump at 286.7 eV observed between the π^* and the σ^* bonds is attributed to the C-H bond,[18] which was presumed to originate from the absorption of hydrocarbon at grain boundaries during the film deposition process.[19] On the other hand, for the $UNCD_{10N}$ films grown without bias with growth time of 10 min (curve II, Fig. 2), there appears only a small peak at ∼284.5 eV (π^*-band) and an abrupt rise near 287.5 eV, which indicates that the films contain only the sp^2 phase. The peaks corresponding to diamond phase are not observable. Only when the UNCD films were grown without bias for longer time, i.e., more than 30 min, the signature of sp^3-bonded carbon, the σ^* bonds at 289.5 eV, and the deep valley at 302 eV were observable (curve III, Fig. 2). These results indicate that in nucleation process without bias, sp^2-bonded carbon was only formed in the first 10 min and no sp^3-bonded carbon was observable. In contrast, by applying bias voltage of −200 V, the diamond grains can be

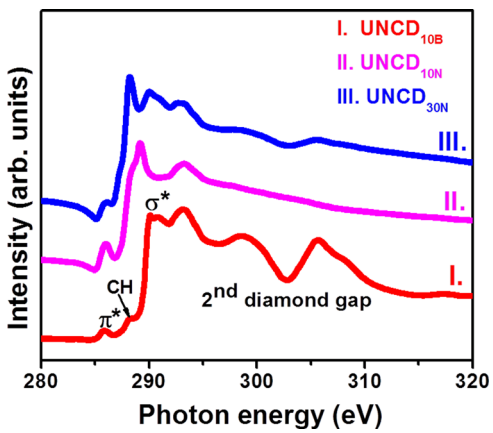

FIG. 2. NEXAFS spectra of (I) $UNCD_{10B}$, (II) $UNCD_{10N}$, and (III) $UNCD_{30N}$ films.

This article is copyrighted as indicated in the article. Reuse of AIP content is subject to the terms at: http://scitation.aip.org/termsconditions. Downloaded to IP: 163.13.36.166 On: Fri, 12 Dec 2014 02:24:24

initiated at the very beginning of the film's growth in CH_4/Ar plasma.

The EFE properties of these UNCD films were measured with a tunable parallel plate setup, in which the cathode-to-anode distance was controlled using a micrometer. The current-voltage (I-V) characteristics were measured using an electrometer (Keithley 2410) under 10^{-6} Torr and were modeled by Fowler-Nordheim (F-N) theory.[20] Fig. 3 shows the EFE properties, the current density (J_e) versus applied field (E) curves, of the films deposited in CH_4/Ar plasma with or without bias. The corresponding F-N plots, the log (J_e/E^2) versus $1/E$ curves, were shown as the inset in Fig. 3. The turn-on field (E_0) was designated as the point of interception of the straight lines extrapolated from the low and the high-field segments of the F-N plots. Interestingly, the $UNCD_{10B}$ films possess the best EFE properties, viz., the lowest E_0 value of 4.2 V/μm and the highest J_e value of 2.6 mA/cm^2 at E = 8.5 V/μm (curve I, Fig. 3). In contrast, the EFE properties were inferior when the UNCD films were grown without bias. Curve II of Fig. 3 shows that the E_0 value was increased to (E_0) = 10.8 V/μm with the J_e value of 2.2 mA/cm^2 at $E = 17.8$ V/μm for $UNCD_{10N}$ films and curve III of Fig. 3 shows that (E_0) = 16.6 V/μm and (J_e) = 1.3 mA/cm^2 at $E = 27.6$ V/μm for $UNCD_{30N}$ films.

The above-described results generate two unresolved questions concerning the role of negative bias voltage on the evolution of granular structure and the EFE behavior of the UNCD films; they are: (i) what are the grain boundary phases formed during the fast growth of $UNCD_{10B}$ films? and (ii) how do they enhance the EFE properties of $UNCD_{10B}$ films? To answer these questions, TEM microstructural investigations (Jeol 2100F) were performed to verify the changes of the hybridized carbon phase in the films. It should be noted that when the samples were ion-milled only from the Si side, the TEM foil contains mostly the regions near the surface of the UNCD films, whereas when the samples were ion-milled both from the top and the bottom surfaces evenly at the same time, the thin foil will contain the materials near the UNCD-to-Si interface of the UNCD films. The bright field (BF) TEM image for the surface region of $UNCD_{10B}$ films (Fig. 4(a)) and the associated selected area electron diffraction (SAED) pattern (inset, Fig. 4(a)) show that the clusters in the film consist of ultra-small spherical diamond grains (5–10 nm). Detailed examination of the SAED patterns reveals the commonly observed (111), (220), and (311) diffraction rings corresponding to the structure of diamond phase. Fig. 4(b) shows the TEM micrograph of the interface region of the $UNCD_{10B}$ films, indicating that this region of the films show similar granular structure as those observed in the surface region of the films (cf. Fig. 4(a)), i.e., there are evenly distributed ultranano-sized diamond grains. The corresponding SAED pattern of Fig. 4(b) also reveals the usually observed (111), (220), and (311) diffraction rings corresponding to the structure of diamond phase.

On the other hand, the BF-TEM image for the surface region of $UNCD_{10N}$ (Fig. 4(c)) along with the SAED pattern (inset of Fig. 4(c)) shows that the films also consist of ultra-small spherical diamond grains as like the grains in the surface region of $UNCD_{10B}$ films. Nevertheless, the TEM micrograph corresponding to the interface region of the $UNCD_{10N}$ films (Fig. 4(d)) shows a faint micrograph of undeveloped diamond grains. The SAED pattern shown in the inset of Fig. 4(d) also shows a large diffused ring in the center of the SAED along with the faded diamond rings, signifying the existence of amorphous (or sp^2-bonded) phase in this region with fewer diamond grains. These TEM observations clearly evidenced that diamond grains were formed at the very beginning of the film's growth for $UNCD_{10B}$ films due to applied bias, whereas only *a-C* phase were present at the interface region for the $UNCD_{10N}$ films grown without bias.

The behavior of the applied negative bias voltage on modifying the microstructure of the UNCD films is

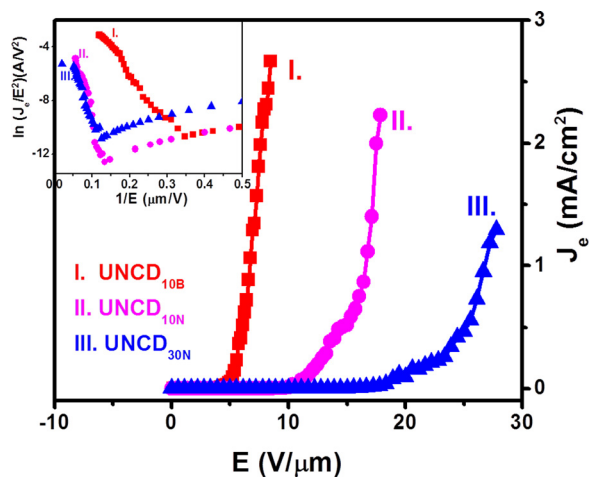

FIG. 3. EFE properties of (I) $UNCD_{10B}$, (II) $UNCD_{10N}$, and (III) $UNCD_{30N}$ films. The inset shows the corresponding F-N plots.

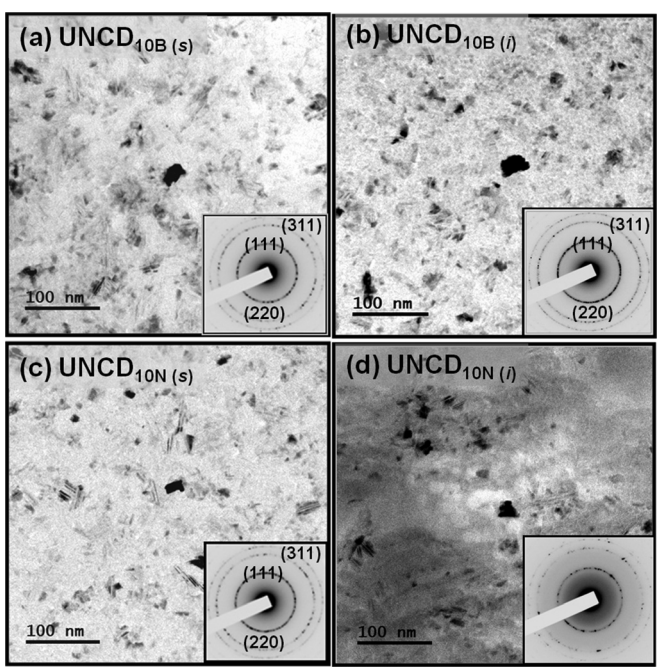

FIG. 4. The TEM bright field micrographs of (a) the surface region and (b) the interface region of $UNCD_{10B}$ films with the insets showing the SAED patterns of the corresponding TEM images. The TEM bright field micrographs of (c) the surface region and (d) the interface region of $UNCD_{10N}$ films with the insets showing the SAED patterns of the corresponding TEM images.

This article is copyrighted as indicated in the article. Reuse of AIP content is subject to the terms at: http://scitation.aip.org/termsconditions. Downloaded to IP: 163.13.36.166 On: Fri, 12 Dec 2014 02:24:24

interesting, but such information is not able to account for the significant improvement on the EFE properties for the $UNCD_{10B}$ films. To understand the genuine mechanism on the enhancement of these properties, the bonding structure of the UNCD films was examined using the carbon K-edge electron energy loss spectroscopy (EELS) to unambiguously distinguish between the different carbon materials such as diamond, graphite and *a-C*.[21] Fig. 5 shows the selected area EELS spectra corresponding to each TEM micrograph of $UNCD_{10B}$ and $UNCD_{10N}$ films (cf. Fig. 4), revealing that there are significant changes in bonding structure due to the application of negative bias voltage in the nucleation and the growth process. The carbon edge core-loss EELS spectra corresponding to both the surface and the interface regions of $UNCD_{10B}$ films (curves I and II, respectively, Fig. 5(a)) and that of $UNCD_{10N}$ films (curves III and IV, respectively, Fig. 5(a)) contain an abrupt rise near 289.5 eV (σ*-band) and a large dip in the vicinity of 302 eV, implying the diamond nature of the materials[22,23] in both the $UNCD_{10B}$ and the $UNCD_{10N}$ films. But the signature of sp^3-bonded carbons in the interface region of $UNCD_{10N}$ films is much less prominent, compared to that in the surface region of the films. There is a π*-band at 285.5 eV in core-loss EELS spectra, indicating that some proportion of sp^2-bonded carbon was induced, probably along the grain boundary regions of these UNCD films.

It is still necessary to differentiate the nature of the sp^2-bonded carbon to understand the genuine mechanism for enhancing the EFE properties for the $UNCD_{10B}$ films.

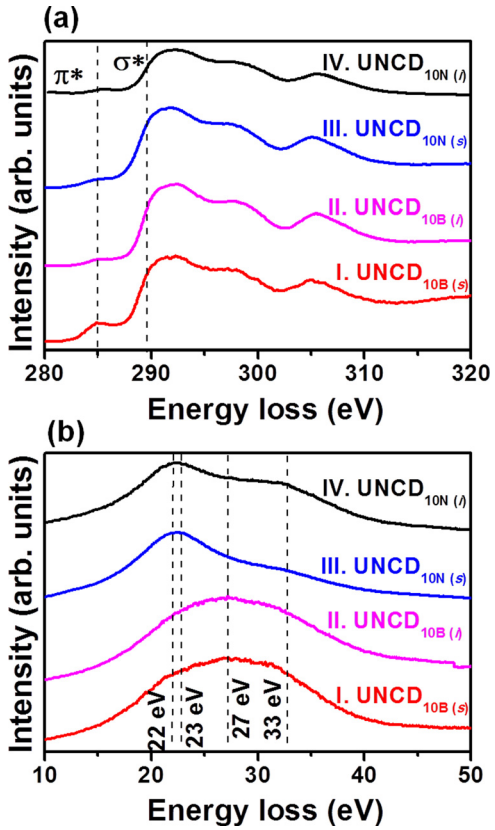

FIG. 5. Selected area EELS spectra for surface region (designated as "*s*") and interface region (designated as "*i*") of $UNCD_{10B}$ or $UNCD_{10N}$ films; (a) core-loss EELS spectra and (b) plasmon-loss EELS spectra for (I) $UNCD_{10B(s)}$, (II) $UNCD_{10B(i)}$, (III) $UNCD_{10N(s)}$, and (IV) $UNCD_{10N(i)}$.

Notably, the plasmon-loss EELS spectra are the most effective measurement for distinguishing the crystalline sp^2-bonded carbons (the graphite) from the amorphous ones, as the plasmon-loss EELS spectra for the graphitic phase shows a prominent peak at s_3 (27 eV) and those for the *a-C* phase shows a peak at s_1 (22 eV).[23,24] In contrast, the crystalline sp^3-bonded carbons in diamond, shows a peak consequent to the bulk plasmon at s_4 (33 eV) with a shoulder corresponding to the surface plasmon at s_2 (23 eV). The I_{s2}/I_{s4} ratio is about $1:\sqrt{2}$. Curves I and II in Fig. 5(b) show the plasmon-loss EELS spectra of the surface and the interface regions of $UNCD_{10B}$ films, respectively. It is observed that both the surface and the interface regions of $UNCD_{10B}$ films are dominated by larger s_3-band ($\sim$27 eV) along with the s_2- and s_4-bands,[25] indicating that both regions consist of some proportion of graphitic phases besides diamond. Quite the opposite, the plasmon-loss spectra for both the surface and the interface regions of $UNCD_{10N}$ (curves III and IV, respectively, Fig. 5(b)) are subjugated by s_1-band (22 eV), in which s_2- and s_4-bands are still present but with much smaller spectral weight compared with the s_1-band (22 eV). These results indicate that the films grown without bias possess *a-C* phases along with some diamond grains in the UNCD films. Such a result is in accord with the previous observations that the bias enhanced growth of UNCD films induced the formation of graphitic phases in the grain boundary regions of the UNCD films.[9,10] Moreover, Teng *et al.* also reported the induction of nano-graphite filaments, when the diamond films were grown in CH_4/H_2 plasma using bias voltage.[11] Previous reports revealed that the graphitic phases are more conducting than that of the *a-C* phases,[25,26] such that the formation of sp^2-bonded graphitic phases at the grain boundaries creates conduction channels for the electrons.

In summary, in this work, the films were grown by BEN-BEG process in CH_4/Ar plasma. The application of negative bias voltage not only induced the instantaneous nucleation of diamond circumventing the formation of *a-C* phase near the UNCD-to-Si interface region but also converted the grain boundary phase into nanographite. Hence, the electrons can be transported easily across the UNCD-to-Si interface and along the graphite phases to the emitting surface, and which were then emitted to vacuum without any difficulty. Especially, $UNCD_{10B}$ films exhibited superior EFE properties as $E_0 = 4.2\,V/\mu m$ with $J_e = 2.6\,mA/cm^2$ at $E = 8.5\,V/\mu m$. On the other hand, the $UNCD_{10N}$ films contain mostly the *trans*-polyacetylene phases in the grain boundaries and *a-C* phase in the interface, resulting in inferior EFE properties. As a result, the fast growth process of UNCD films using negative bias voltage induced graphitic phase in the grain boundaries, which is the genuine factor for the superior EFE properties of $UNCD_{10B}$ films.

The authors like to thank the financial support of National Science Council, Taiwan through the Project No. NSC 102-2112-M-032 -006.

[1]J. E. Field, *The Properties of Diamonds* (Academic, London, 1979).
[2]H. Liu and D. S. Dandy, Diamond Relat. Mater. **4**, 1173 (1995).
[3]J. C. Angus, H. A. Will, and W. S. Stanko, J. Appl. Phys. **39**, 2915 (1968).

This article is copyrighted as indicated in the article. Reuse of AIP content is subject to the terms at: http://scitation.aip.org/termsconditions. Downloaded to IP: 163.13.36.166 On: Fri, 12 Dec 2014 02:24:24

[4]S. Jiao, A. Sumant, M. A. Kirk, D. M. Gruen, A. R. Krauss, and O. Auciello, J. Appl. Phys. **90**, 118 (2001).
[5]D. Zhou, A. R. Krauss, L. C. Qin, T. G. McCauley, D. M. Gruen, T. D. Corrigan, R. P. H. Chang, and H. Gnaser, J. Appl. Phys. **82**, 4546 (1997).
[6]K. J. Sankaran, P. T. Joseph, H. C. Chen, N. H. Tai, and I. N. Lin, Diamond Relat. Mater. **20**, 232 (2011).
[7]T. H. Chang, K. Panda, B. K. Panigrahi, S. C. Lou, C. Chen, H. C. Chen, I. N. Lin, and N. H. Tai, J. Phys. Chem. C **116**, 19867 (2012).
[8]Y. C. Chu, C. H. Tu, C. P. Liu, Y. Tzeng, and O. Auciello, J. Appl. Phys. **112**, 124307 (2012).
[9]Y. C. Chen, X. Y. Zhong, A. R. Konicek, D. S. Grierson, N. H. Tai, I. N. Lin, B. Kabius, J. M. Hiller, A. V. Sumant, R. W. Carpick, and O. Auciello, Appl. Phys. Lett. **92**, 133113 (2008).
[10]X. Y. Zhong, Y. C. Chen, N. H. Tai, I. N. Lin, J. M. Hiller, and O. Auciello, J. Appl. Phys. **105**, 034311 (2009).
[11]K. Y. Teng, H. C. Chen, G. C. Tzeng, C. Y. Tang, H. F. Cheng, and I. N. Lin, J. Appl. Phys. **111**, 053701 (2012).
[12]K. J. Sankaran, K. Srinivasu, H. C. Chen, C. L. Dong, K. C. Leou, C. Y. Lee, N. H. Tai, and I. N. Lin, J. Appl. Phys. **114**, 054304 (2013).
[13]J. Birrell, J. E. Gerbi, O. Auciello, J. M. Gibson, D. M. Gruen, and J. A. Carlisle, J. Appl. Phys. **93**, 5606 (2003).
[14]Y. K. Chang, H. H. Hsieh, W. F. Pong, M. H. Tsai, F. Z. Chien, P. K. Tseng, L. C. Chen, T. Y. Wang, K. H. Chen, J. R. Bhusari, J. R. Yang, and S. T. Lin, Phys. Rev. Lett. **82**, 5377 (1999).
[15]P. T. Joseph, N. H. Tai, C. H. Chen, H. Niu, H. F. Cheng, W. F. Pong, and I. N. Lin, J. Phys. D: Appl. Phys. **42**, 105403 (2009).
[16]J. Nithianandam, J. C. Rife, and H. Windischmann, Appl. Phys. Lett. **60**, 135 (1992).
[17]A. Gutierrez, M. F. Lopez, I. Garcia, and A. Vazquez, J. Vac. Sci. Technol., A **15**, 294 (1997).
[18]S. S. Chen, H. C. Chen, W. C. Wang, C. Y. Lee, I. N. Lin, J. Guo, and C. L. Chang, J. Appl. Phys. **113**, 113704 (2013).
[19]L. Ponsonnet, C. Donnet, K. Varlot, J. M. Martin, A. Grill, and V. Patel, Thin Solid Films **319**, 97 (1998).
[20]R. H. Fowler and L. Nordheim, Proc. R. Soc. London, Ser. A **119**, 173 (1928).
[21]A. Dato, V. Radmilovic, Z. Lee, J. Philips, and M. Frenklach, Nano. Lett. **8**, 2012 (2008).
[22]D. M. Gruen, S. Liu, A. R. Krauss, J. Luo, and X. Pan, Appl. Phys. Lett. **64**(12), 1502 (1994).
[23]P. Kovarik, E. B. D. Bourdon, and R. H. Prince, Phys. Rev. B **48**, 12123 (1993).
[24]I. Jimenez, M. M. Garcia, J. M. Albella, and L. J. Terminello, Appl. Phys. Lett. **73**, 2911 (1998).
[25]K. J. Sankaran, J. Kurian, H. C. Chen, C. L. Dong, C. Y. Lee, N. H. Tai, and I. N. Lin, J. Phys. D: Appl. Phys. **45**, 365303 (2012).
[26]K. Y. Teng, H. C. Chen, H. Y. Chiang, C. C. Horng, H. F. Cheng, K. J. Sankaran, N. H. Tai, C. Y. Lee, and I. N. Lin, Diamond Relat. Mater. **24**, 126 (2012).

This article is copyrighted as indicated in the article. Reuse of AIP content is subject to the terms at: http://scitation.aip.org/termsconditions. Downloaded to IP: 163.13.36.166 On: Fri, 12 Dec 2014 02:24:24